Achievements and open issues in the determination of Parton Distributions and Fragmentation Functions

Synergies of pp and pA Collisions with an Electron-Ion Collider

Emanuele R. Nocera

Rudolf Peierls Centre for Theoretical Physics - University of Oxford

Brookhaven National Laboratory - June 26 2017

1. Foreword

Factorisation of physical observables [Adv.Ser.Direct.HEP 5 (1988) 1]

1. A variety of sufficiently inclusive processes allow for a factorised description

short-distance part		long-distance part
hard interaction of partons	$\xleftrightarrow[\text{scheme \& scale } \mu]{\text{factorisation}}$	nucleon structure
process-dependent kernels		universal parton distributions

2. Physical observables are written as a convolution of coefficient functions and PDFs

$$\mathcal{O}_I = \sum_{f=q,\bar{q},g} C_{If}(y, \alpha_s(\mu^2)) \otimes f(y, \mu^2) + \text{p.s. corrections} \qquad f \otimes g = \int_x^1 \frac{dy}{y} f\left(\frac{x}{y}\right) g(y)$$

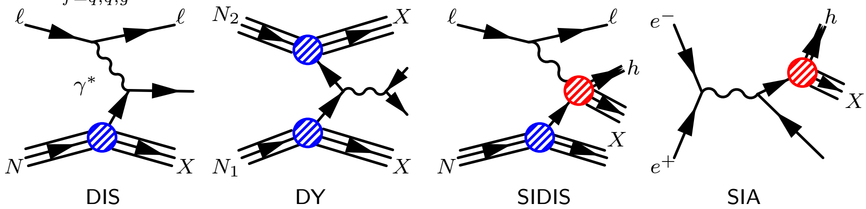

3. Coefficient functions allow for a perturbative expansion

$$C_{If}(y, \alpha_s) = \sum_{k=0} a_s^k C_{If}^{(k)}(y), \qquad a_s = \alpha_s/(4\pi)$$

4. After factorisation, all quantities (including PDFs/FFs) depend on μ

Field-theoretic definition on the light-cone [Rev.Mod.Phys. 67 (1995) 157]

Parton Distribution functions (PDFs)

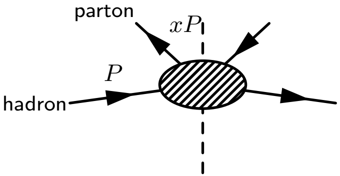

collinear transition of a massles hadron h into a massless parton i with fractional momentum x

local OPE $\Longrightarrow$ lattice formulation

Fragmentation Functions (FFs)

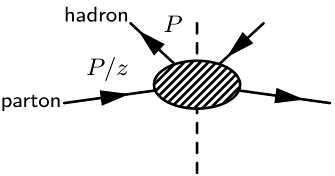

collinear transition of a massless parton i into a massless hadron h with fractional momentum z

no local OPE $\Longrightarrow$ no lattice formulation

Expectation values (matrix elements) of certain (bilocal) operators in hadronic states

$$f_i^h(x) = \frac{1}{4\pi}\int dy^- e^{-ixP^+y^-}\langle h(P)|\bar{\psi}_i(0,y^-,\mathbf{0}_\perp)\gamma^+\mathcal{P}\psi_i(0)|h(P)\rangle$$

$$D_i^h(z) = \frac{1}{12\pi}\sum_X\int dy^- e^{i\frac{P^+}{z}y^-}\,\mathrm{Tr}\left[\gamma^+\langle 0|\psi(0,y,\mathbf{y}_\perp)\mathcal{P}|h(P)\,X\rangle\langle h(P)\,X|\mathcal{P}'\bar{\psi}(0)|0\rangle\right]$$

$$y = (y^+,y^-,\mathbf{y}_\perp)\,,\qquad y^+ = (y^0+y^z)/\sqrt{2}\,,\qquad y^- = (y^0-y^z)/\sqrt{2}\,,\qquad \mathbf{y}_\perp = (y^x,y^y)$$

All these definitions have ultraviolet divergences which must be renormalized to define finite PDFs and FFs to be used in the factorisation formulas

(PDF/FFs are scheme dependent)

All these definitions can be generalised to include longitudinal/transverse polarizations

A global determination of parton distribution functions

A mathematically ill-posed problem: determine a set of functions from a finite set of data

METHODOLOGY

1. Parametrisation: general, smooth, flexible at an initial scale Q_0^2

$$xf_i(x,Q_0^2) = A_{f_i}\, x^{a_{f_i}}\, (1-x)^{b_{f_i}}\, \mathscr{F}(x,\{c_{f_i}\})$$

small x		large x
$xf_i(x,Q^2) \xrightarrow{x\to 0} x^{a_{f_i}}$	$\mathscr{F}(x,\{c_{f_i}\}) \underset{x\to 1}{\xrightarrow{x\to 0}} \text{finite}$ $\xrightarrow[\text{smooth interpolation in between}]{}$	$xf_i(x,Q^2) \xrightarrow{x\to 1} (1-x)^{b_{f_i}}$
(Regge theory)	(polynomials, neural networks)	(quark counting rules)

2. A prescription to determine/compute expectation values and uncertainties

$$E[\mathcal{O}] = \int \mathcal{D}\Delta f \mathcal{P}(\Delta f|data)\mathcal{O}(\Delta f) \qquad V[\mathcal{O}] = \int \mathcal{D}\Delta f \mathcal{P}(\Delta f|data)[\mathcal{O}(\Delta f) - E[\mathcal{O}]]^2$$

Monte Carlo: $\mathcal{P}(\Delta f|data) \longrightarrow \{\Delta f_k\}$

$$E[\mathcal{O}] \approx \tfrac{1}{N}\textstyle\sum_k \mathcal{O}(\Delta f_k)$$

$$V[\mathcal{O}] \approx \tfrac{1}{N}\textstyle\sum_k [\mathcal{O}(\Delta f_k) - E[\mathcal{O}]]^2$$

Maximum likelihood: $\mathcal{P}(\Delta f|data) \longrightarrow \Delta f_0$

$$E[\mathcal{O}] \approx \mathcal{O}(\Delta f_0)$$

$$V[\mathcal{O}] \approx \text{Hessian}, \Delta\chi^2 \text{envelope}, \ldots$$

COMBINED WITH THEORY AND DATA TO FIND BEST-FIT PDFs

2. Parton Distribution Functions

The role of PDF uncertainties

[CERN Yellow report, 1610.07922]

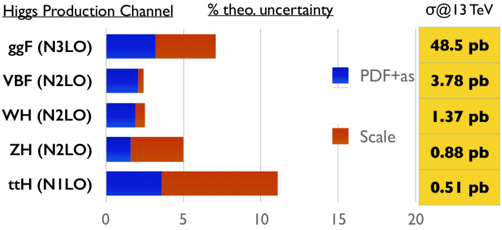

1. Higgs boson characterization
   PDF uncertainty often dominant contribution to theory uncertainty
2. Determination of SM parameters
   PDF uncertainty largest theoretical uncertainty in M_W determination
3. BSM gluino production
   the larger the mass of the final state the larger the PDF uncertainty

[PRD 91 (2015) 113005]

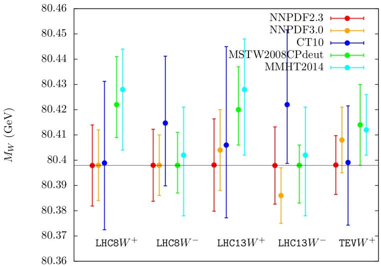

[EPJ C76 (2016) 53]

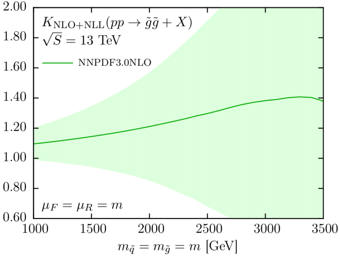

Overview of recent PDF determinations

	NNPDF3.1	MMHT2014	CT14	HERAPDF2.0	CJ15	ABMP16
Fixed target DIS	☑	☑	☑	☒	☑	☑
JLAB	☒	☒	☒	☒	☑	☒
HERA I+II	☑	☑	☑	☑	☑	☑
HERA jets	☒	☑	☒	☒	☒	☒
Fixed target DY	☑	☑	☑	☒	☑	☑
Tevatron W, Z	☑	☑	☑	☒	☑	☑
Tevatron jets	☑	☑	☑	☒	☑	☒
LHC jets	☑	☑	☑	☒	☒	☒
LHC vector boson	☑	☑	☑	☒	☒	☑
LHC top (incl.)	☑	☒	☒	☒	☒	☒
LHC (diff.)	☑	☒	☒	☒	☒	☒
statistical treatment	Monte Carlo	Hessian $\Delta\chi^2$ dynamical	Hessian $\Delta\chi^2$ dynamical	Hessian $\Delta\chi^2=1$	Hessian $\Delta\chi^2=1.645$	Hessian $\Delta\chi^2=1$
parametrisation	Neural Network (259 pars)	Chebyschev pol. (37 pars)	Bernstein pol. (30-35 pars)	polynomial (14 pars)	polynomial (24 pars)	polynomial (15 pars)
HQ scheme	FONLL	TR$'$	ACOT-χ	TR$'$	ACOT-χ	FFN
latest update	1706.00428	EPJ C75 (2015) 204	PRD 89 (2014) 033009	EPJ C75 (2015) 580	PRD 93 (2016) 114017	1701.05838

See also recommendations for PDF usage
in computations of (LHC) high-energy processes [JPG 43 (2016) 023001, EPJC 76 (2016) 471]

A plethora of new data

1. GLUON
   inclusive jets and dijets (medium/large x)
   isolated photon and γ+jets (medium/large x)
   top pair production (large x)
   high p_T V production (small/medium x)
2. QUARKS
   high $p_T W$(+ jets) ratios (medium/large x)
   W and Z production (medium x)
   low and high mass DY (small and large x)
   $W + c$ (strange at medium x)
3. PHOTON
   low and high mass DY
   WW production
4. Great progress also in interface NLO (NNLO) codes to PDF fitting codes
   APPLgrid [EPJ C66 (2010) 503]
   FASTNLO [Kluge et al., 2010]
   aMCfast [JHEP 1408 (2014) 166]
   MCgrid [CPC 185 (2014) 2115]
   APFELgrid [CPC 212 (2017) 205]

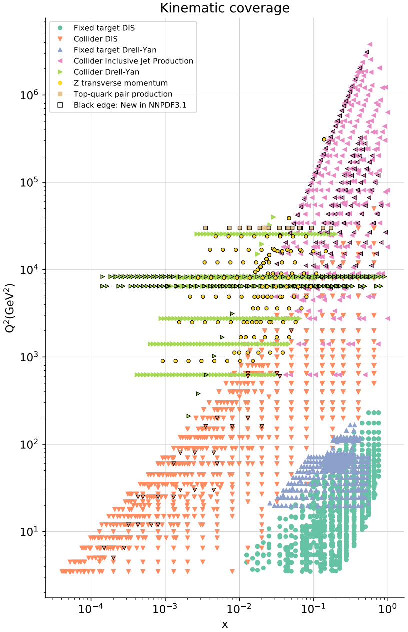

A wealth of new NNLO calculations

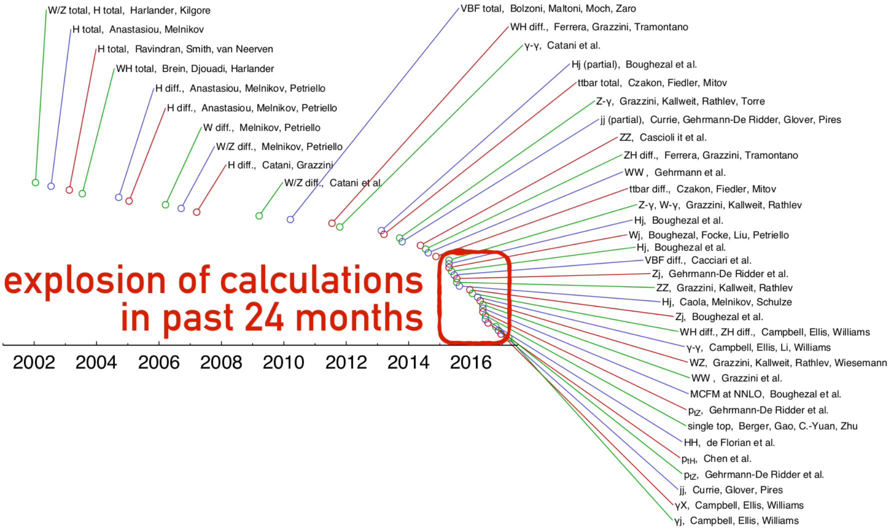

[Slide: courtesy of G. Salam, updated April 2017]

The gluon PDF

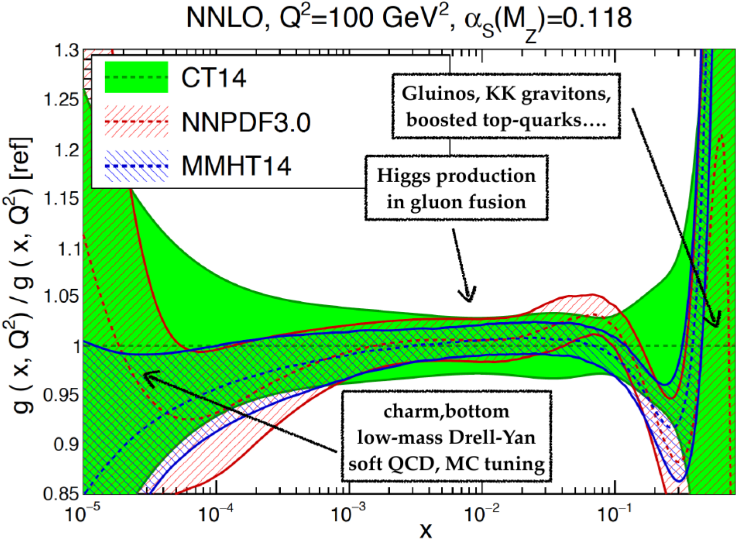

A precise knowledge of the gluon PDF is required over all the range in x to exploit the full potential of the LHC

The gluon PDF at large x: $t\bar{t}$ differential distributions

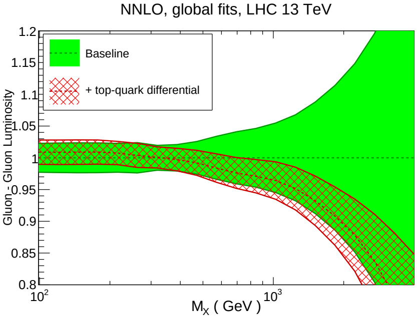

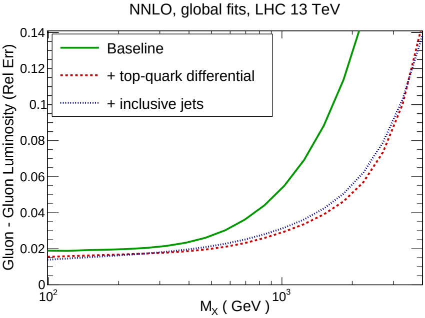

ATLAS and CMS rapidity distributions at $\sqrt{s} = 8$ TeV

Significant reduction of gg luminosity uncertainties at $M_X \geq \mathcal{O}(1)$ TeV

e.g., at $M_X \sim 2$ TeV, uncertainties decrease from 13% to 5%

Impact of $t\bar{t}$ differential data similar to that of jet data

though jet data analysed neglecting NNLO QCD corrections in the matrix element

A precision determination of the gluon PDF at large x is now possible at NNLO

the situation should only improve thanks to the recent NNLO jet calculation

$t\bar{t}$ differential distributions are included in the NNPDF3.1 PDF release

[see JHEP 1704 (2017) 044 and 1706.00428 for details]

The gluon PDF at medium x: the Z-boson p_T distribution

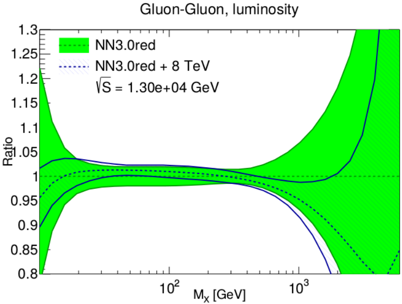

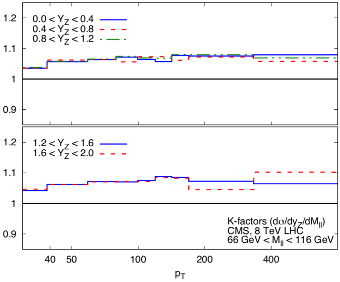

ATLAS and CMS p_T distributions at $\sqrt{s} = 8$ TeV

in various rapidity bins in the Z-peak region

NNLO/NLO K-factors 5%-10% depending on the rapidity/invariant mass region

challenge: measurements have sub-percent experimental errors

Complementary information on the gluon PDF

e.g., at $M_X \sim 2$ TeV, uncertainties decrease from 13% to 8%

Z p_T distributions are included in the NNPDF3.1 PDF release

[see 1705.00343 and 1706.00428 for details]

The gluon PDF at small x: forward charm production

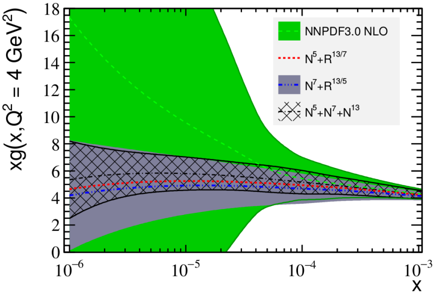

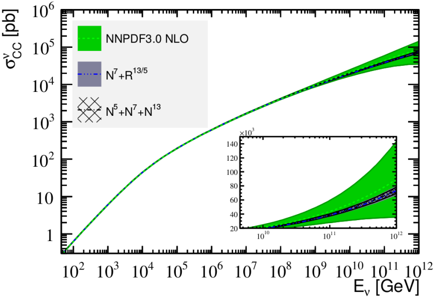

D meson production from LHCb at different center-of-mass energies

$$N_X^{ij} = \frac{d^2\sigma(X\ \text{TeV})}{dy_i^D\, d(p_T^D)_j} \Big/ \frac{d^2\sigma(X\ \text{TeV})}{dy_{\text{ref}}^D\, d(p_T^D)_j} \qquad R_{13/X}^{ij} = \frac{d^2\sigma(13\ \text{TeV})}{dy_i^D\, d(p_T^D)_j} \Big/ \frac{d^2\sigma(X\ \text{TeV})}{dy_i^D\, d(p_T^D)_j}$$

Gluon PDF errors are reduced by up to a factor 10 below $x \sim 10^{-5}$

robust w.r.t theoretical uncertainties (charm mass, scale variations, alternative reference bins)

Combine result with future LHeC measurements of F_L

test for BFKL resummations and non-linear QCD dynamics

Application: ultra high-energy (UHE) neutrino-nucleus cross-sections

NLO QCD provides a prediction accurate to $\lesssim 10\%$ at $E_\nu \simeq 10^{12}$ GeV

[see PRL 118 (2017) 072001 for details]

The NNPDF3.1 upgraded gluon

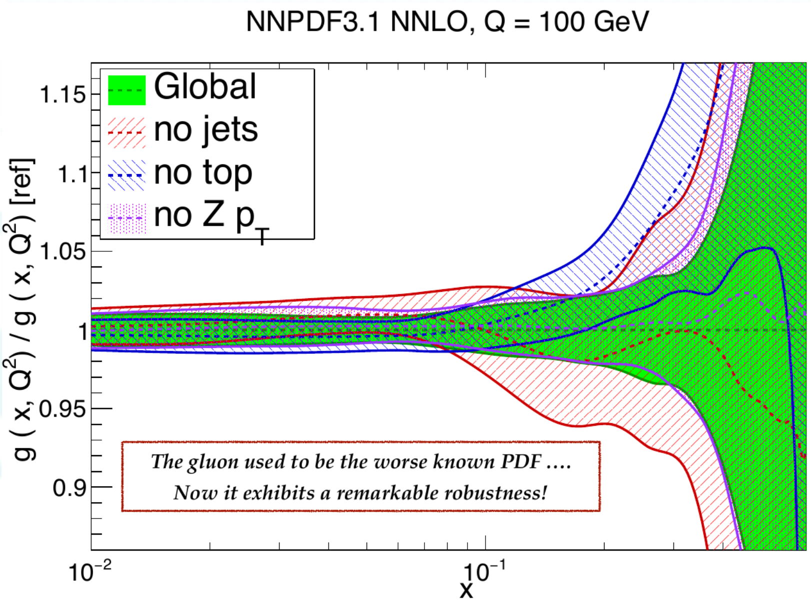

Quark flavour separation from LHC data

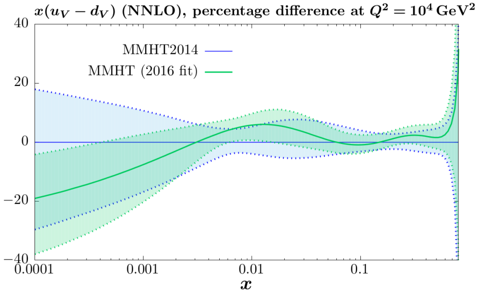

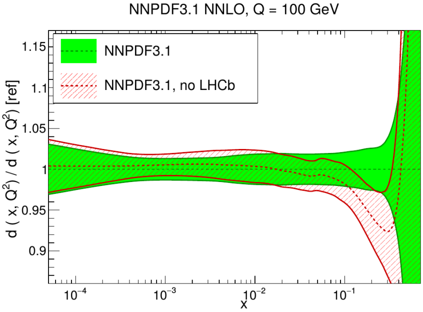

High-precision W and Z production data from ATLAS, CMS and LHCb
handle on quark/antiquark flavour separation

Largest impact on light quarks at large x provided by LHCb data
error reduction by a factor 2 in NNPDF3.1 at $x \sim 0.1$

Combined effect of (LHC) CMS, LHCb and (Tevatron) D0 W, Z data
improved determination of $x(u_V - d_V)$

[see R. Thorne's talk at DIS2017 and 1706.00428 for details]

The PDF ratio d_V/u_V at large x [EPJC 76 (2016) 383]

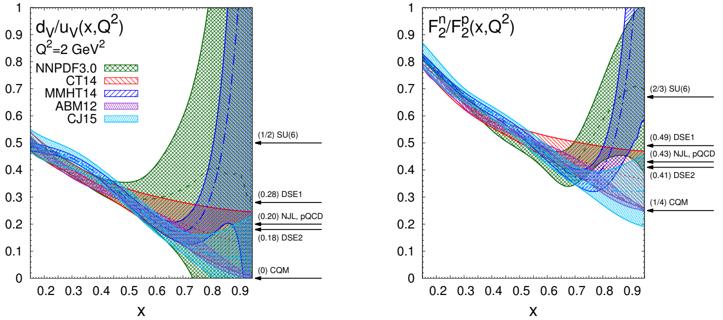

$$\frac{d_V}{u_V} \xrightarrow{x\to 1} (1-x)^{b_{d_V}-b_{u_V}} \xrightarrow[\text{c. r.}]{b_{d_V}=b_{u_V}} k \qquad \frac{F_2^n}{F_2^p} \xrightarrow{x\to 1} \frac{4(1-x)^{b_{u_V}}+(1-x)^{b_{d_V}}}{(1-x)^{b_{u_V}}+4(1-x)^{b_{d_V}}} \xrightarrow[\text{c. r.}]{b_{d_V}=b_{u_V}} 1$$

$$\text{case } b_{u_V} \gg b_{d_V}: \ \frac{d_V}{u_V} \xrightarrow{x\to 1} \infty; \ \frac{F_2^n}{F_2^p} \xrightarrow{x\to 1} 4 \qquad \text{case } b_{u_V} \ll b_{d_V}: \ \frac{d_V}{u_V} \xrightarrow{x\to 1} 0; \ \frac{F_2^n}{F_2^p} \xrightarrow{x\to 1} \frac{1}{4}$$

No predictive power from current PDF determinations, no discrimination among models unless $\frac{d_V}{u_V} \xrightarrow{x\to 1} k$ is built in the parametrisation (CT14, CJ16, ABM12)

The EIC may measure the ratio F_2^n/F_2^p with high accuracy, provided neutron beams expected to be less prone to nuclear and/or higher twist corrections than fixed-target DIS

Complementary measurements from the LHC (DY) and (particularly) the LHeC (DIS)

The strange PDF from collider data

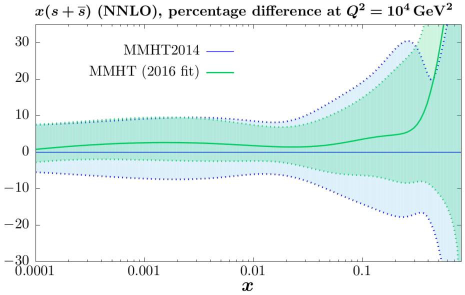

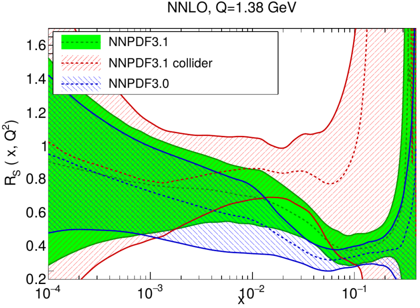

In most PDF fits the strange PDF is suppressed w.r.t up and down sea quark PDFs
effect mostly driven by neutrino dimuon data

A symmetric strange sea PDF is preferred by recent collider data
in particular by ATLAS W, Z rapidity distributions (2011)

$$R_s(x,Q^2) = \frac{s(x,Q^2)+\bar{s}(x,Q^2)}{\bar{u}(x,Q^2)+\bar{d}(x,Q^2)} \begin{cases} \sim 0.5 \text{from neutrino and CMS } W+c \text{ data} \\ \sim 1.0 \text{from ATLAS } W, Z \end{cases}$$

The new ATLAS data can be accommodated easily in the global fit
increased strangeness, though not as much as in a collider-only fit
some tension remains between collider and neutrino data

[see R. Thorne's talk at DIS2017 and 1706.00428 for details]

The strange content of the proton

$$R_S = (s + \bar{s}) / (\bar{u} + \bar{d})$$

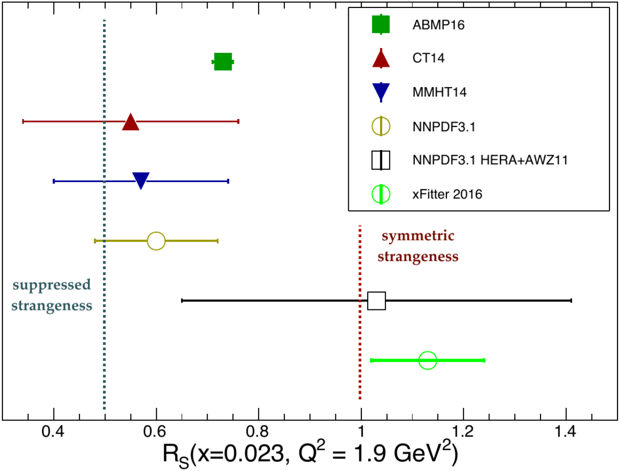

In a global fit the strange content of the proton results from the various pulls of all the different experiments

More strange-sensitive measurements are needed to shed light on it

The strange PDF: $K^{\pm}$ production in SIDIS at an EIC

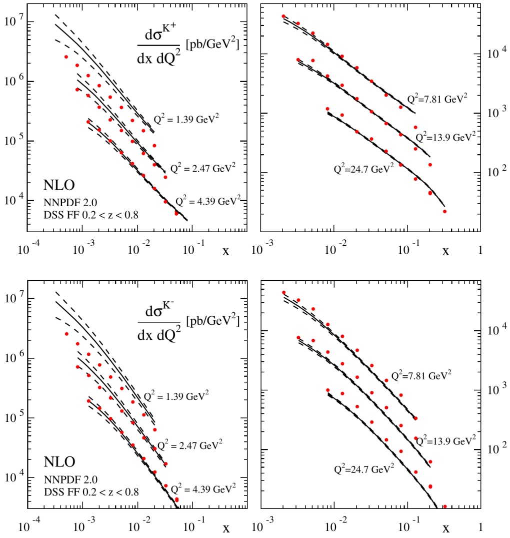

[figure taken from arXiv:1108:1713]

red points: pseudodata at an EIC (based on PYTHIA + JETSET)

black curves: theory predictions (NNPDF2.0 + DSS07, NLO)

$0.01 \leq y \leq 0.95$, $\sqrt{s} = 70.7$ GeV
z integrated in the range $[0.2, 0.8]$

small x: $d\sigma^{K^+} \approx d\sigma^{K^-}$
large x: $d\sigma^{K^+} \gg d\sigma^{K^-}$
may constrain s^+ and s^-

drawback: $K^{\pm}$ fragmentation
a) study FFs separately
b) analyze PDFs and FFs simultaneously

LHeC: direct sensitivity to s
charm tagging in CC DIS ($W + s \to c$)

$\pi^{\pm}$ production in SIDIS at an EIC allow for a determination of $\bar{u} - \bar{d}$

The charm PDF: perturbative vs fitted

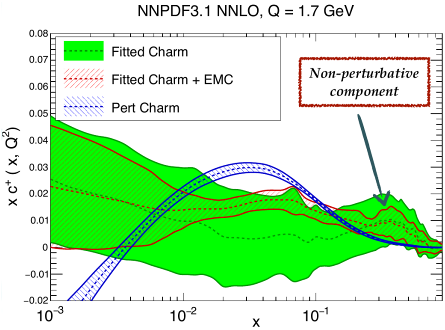

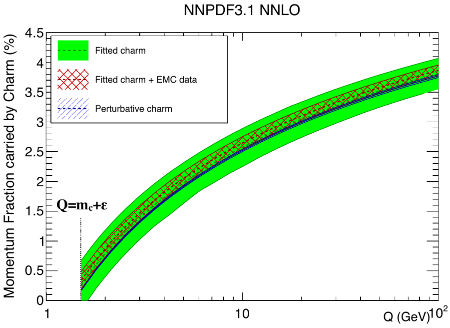

Parametrise the $c^+(x, Q_0^2)$, quark and gluon PDFs on the same footing

stabilise the dependence of LHC processes upon variations of m_c

quantify the nonperturbative charm component in the proton (BHPS? sea-like?)

take into account massive charm-initiated contribution to the DIS structure functions

Fitted charm found to differ from perturbative charm at scales $Q \sim m_c$ in NNPDF3.1

preference for a BHPS-like shape

shape driven by LHCb W, Z data + EMC data

At $Q = 1.65$ GeV charm carry 0.26 ± 0.42 % of the proton momentum

but it is affected by large uncertainties, especially if no EMC data are included

The photon PDF: how bright is the proton? [PRL 117 (2016) 242002]

The photon PDF $\boldsymbol{\gamma}(x,Q)$ *in* ***LUXqed***

$$x f_{\gamma/p}(x,\mu^2) = \frac{1}{2\pi\alpha(\mu^2)} \int_x^1 \frac{dz}{z} \left\{ \int_{\frac{x^2 m_p^2}{1-z}}^{\frac{\mu^2}{1-z}} \frac{dQ^2}{Q^2} \alpha^2(Q^2) \left[\left(z p_{\gamma q}(z) + \frac{2x^2 m_p^2}{Q^2} \right) F_2(x/z, Q^2) - z^2 F_L\left(\frac{x}{z}, Q^2\right) \right] - \alpha^2(\mu^2) z^2 F_2\left(\frac{x}{z}, \mu^2\right) \right\}$$

Good agreement with NNPDF3.0QED, model-independent fit from LHC DY data

$\boldsymbol{\gamma}(x,Q)$*, ratio to* ***LUXqed***

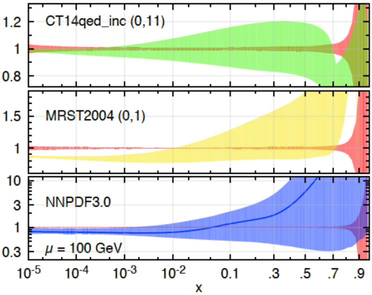

Electroweak corrections become relevant within current precision

especially at large invariant mass

Inclusion of electroweak corrections require a photon PDF

NNPDF2.3QED: first model-independent determination of $\gamma(x,Q)$ from LHC W,Z data

affected by large uncertainties, $\mathcal{O}(100\%)$ due to limited experimental information

LUXQED: compute $\gamma(x,Q)$ in terms of inclusive structure functions F_2 and F_L

significant improvement in the PDF uncertainty

implications for high-mass processes for BSM searches, *e.g.* DY production at the TeV scale

Beyond fixed-order accuracy

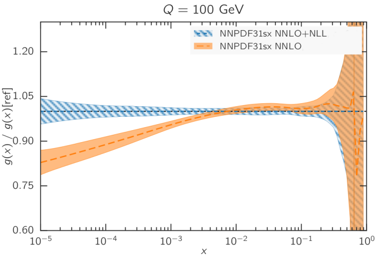

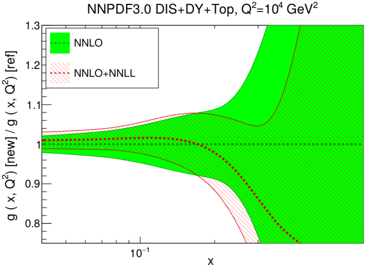

small x: $\frac{1}{x}\ln^k x$

high-energy gluon emission: single logs

large x: $\left(\frac{\ln^k(1-x)}{(1-x)}\right)_+$

soft gluon emission: double logs

Large logs $\alpha_s \ln \sim 1$ spoil the convergence of the perturbative series

PDFs with threshold resummation [JHEP 1509 (2015) 191] (only DIS, DY Z/γ, total $t\bar{t}$)

suppression in PDFs partially or totally compensates enhancements in partonic cross-sections

accuracy of the resummed fit competitive with the fixed-order fit, except for the large-x gluon

large uncertainties for MSSM particle resummed cross-sections [EPJ C76 (2016) 53]

Towards PDFs with high-energy resummation [NNPDF, in progress] (DIS only)

$N_{\rm dat}$	NLO+NLL	NLO	NNLO+NLL	NNLO
3102	1.111	1.113	1.108	1.126

Resummed PDFs enhanced at small x, uncertainties reduced

3. Fragmentation Functions and Helicity PDFs

Modern sets of FFs/helicity PDFs

	DHESS	HKNS	JAM	NNFF1.0
SIA	☑	☑	☑	☑
SIDIS	☑	☒	☒	☒
PP	☑	☒	☒	☒
statistical treatment	Iterative Hessian 68% - 90%	Hessian $\Delta\chi^2 = 15.94$	Monte Carlo	Monte Carlo
parametrisation	standard	standard	standard	neural network
hadron species	$\pi^\pm$, $K^\pm$, $p/\bar{p}$, $h^\pm$	$\pi^\pm$, $K^\pm$, $p/\bar{p}$	$\pi^\pm$, $K^\pm$	$\pi^\pm$, $K^\pm$, $p/\bar{p}$
latest update	PRD 91 (2015) 014035 PRD 95 (2017) 094019	PTEP 2016 (2016) 113B04	PRD 94 (2016) 114004	1706.07049

	DSSV	NNPDF	JAM	LSS
DIS	☑	☑	☑	☑
SIDIS	☑	☒	☒	☑
PP	☑ (jets,π^0)	☑ (jets,$W^\pm$)	☒	☒
statistical treatment	Lagr. mult. $\Delta\chi^2/\chi^2 = 2\%$	Monte Carlo	Hessian $\Delta\chi^2 = 1$	Hessian $\Delta\chi^2 = 1$
parametrisation	polynomial (23 pars)	neural network (259 pars)	polynomial (10 pars)	polynomial (20 pars)
latest update	PRL 113 (2014) 012001	NPB 887 (2014) 276	PRD 89 (2014) 034025	PRD 91 (2015) 054017

The key asset of a polarised EIC: the kinematic coverage

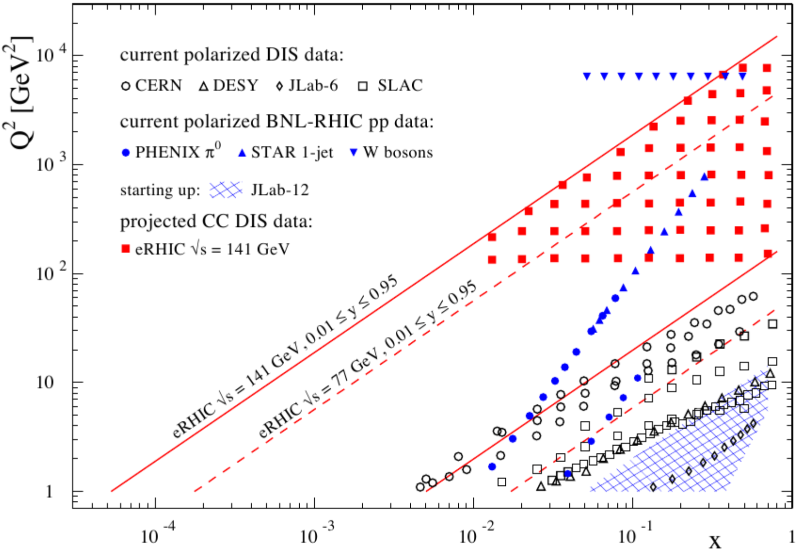

[Figure taken from EPJA 52 (2016) 268]

Projected accuracy at an EIC [PRD 92 (2015) 094030]

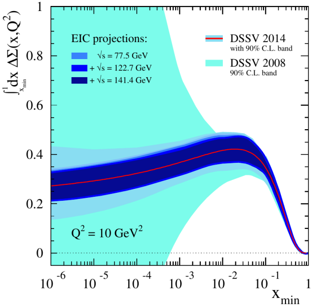

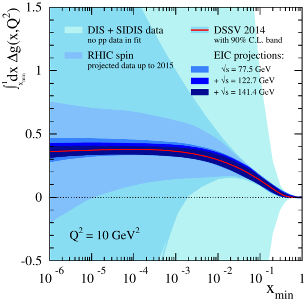

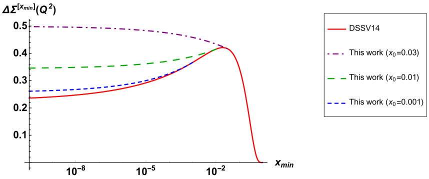

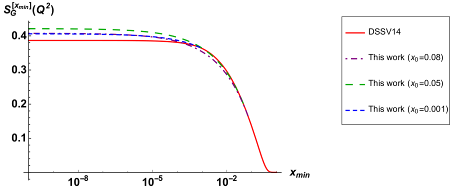

An EIC is expected to control $\Delta\Sigma$ within 15% and Δg within 10% relative accuracy
An EIC may provide an indirect constraint on the orbital angular momentum
Helicity evolution at small x? [More in PRL 118 (2017) 052001, 1706.04236 and Y. Kovchegov's talk]

Impact of new data: di-jet and W-boson production [1702.05077]

Reweighting: NNPDFpol1.1 prior

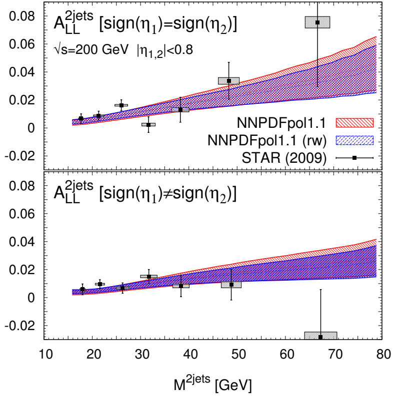

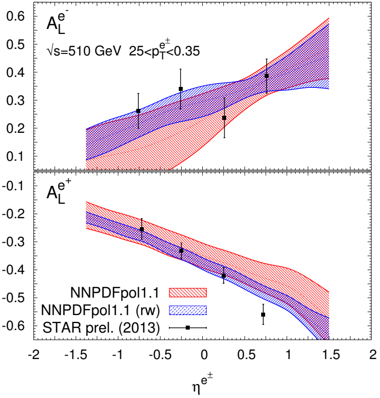

Data set	$\mathcal{L}$ [pb^{-1}]	$\sqrt{s}$ [GeV]	$\mathcal{A}$	$N_{\rm dat}$
STAR09-2j-ss	21	200	$A_{LL}^{\rm 2jets}$	7
STAR09-2j-os	21	200	$A_{LL}^{\rm 2jets}$	7

Data set	$\mathcal{L}$ [pb^{-1}]	$\sqrt{s}$ [GeV]	$\mathcal{A}$	$N_{\rm dat}$
STAR13-W^-	246.2	510	$A_L^{e^-}$	4
STAR13-W^+	246.2	510	$A_L^{e^+}$	4

Impact of new data: di-jet and W-boson production [1702.05077]

Reweighting: NNPDFpol1.1 prior

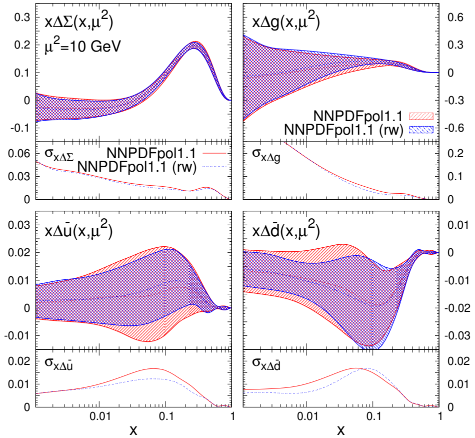

Data set	$N_{\rm dat}$	$\chi^2/N_{\rm dat}$	$\chi^2_{\rm rw}/N_{\rm dat}$
STAR09-2j-ss	7	1.41	1.18
STAR09-2j-os	7	1.26	0.83
STAR13-W^-	4	2.44	0.69
STAR13-W^+	4	3.08	1.30

$$\langle \Delta f(Q^2)\rangle^{[x_{\min},x_{\max}]} \equiv \int_{x_{\min}}^{x_{\max}} dx\, \Delta f(x,Q^2)$$

$$\langle \Delta g(Q^2)\rangle^{[0.01,0.2]} = 0.23 \pm 0.23$$

$$\langle \Delta g(Q^2)\rangle^{[0.01,0.2]}_{\rm rw} = 0.32 \pm 0.21$$

$$Q^2 = 10\ \text{GeV}^2$$

Open issues: SU(3) breaking and strangeness

NNPDFpol1.0 [NPB 874 (2013) 36]
$\int_0^1 dx[\Delta s + \Delta\bar{s}] = -0.13 \pm 0.09$

Lattice [PRL 108 (2012) 222001]
$\int_0^1 dx[\Delta s + \Delta\bar{s}] = -0.020(10)(1)$

First moment constrained by

$$a_3 = \int_0^1 dx[\Delta u^+ - \Delta d^+] = 1.2701 \pm 0.0025$$

$$a_8 = \int_0^1 dx[\Delta u^+ + \Delta d^+ - 2\Delta s^+] = 0.585 \pm 0.025$$

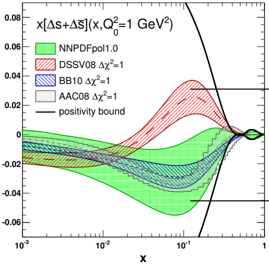

directly from SIDIS Kaon data

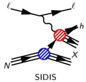

indirectly from DIS + SU(3)

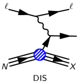

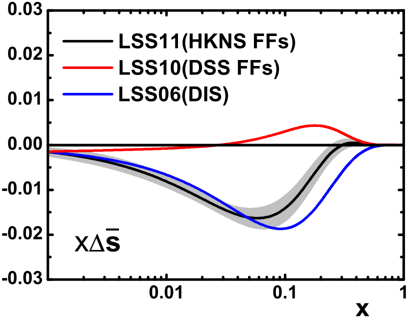

How well do we know Fragmentation Functions?

experiment		data type	norm. N_i	# data in fit	χ^2
TPC [48]		incl.	1.043	17	17.3
		uds tag	1.043	9	2.1
		c tag	1.043	9	5.9
		b tag	1.043	9	9.2
TASSO [49]	34 GeV	incl.	1.043	11	30.2
	44 GeV	incl.	1.043	7	22.2
SLD [19]		incl.	0.986	28	15.3
		uds tag	0.986	17	18.5
		c tag	0.986	17	16.1
		b tag	0.986	17	5.8
ALEPH [16]		incl.	1.020	22	22.9
DELPHI [17]		incl.	1.000	17	28.3
		uds tag	1.000	17	33.3
		b tag	1.000	17	10.6
OPAL [18, 20]		incl.	1.000	21	14.0
		u tag	0.786	5	31.6
		d tag	0.786	5	33.0
		s tag	0.786	5	51.3
		c tag	0.786	5	30.4
		b tag	0.786	5	14.6
BABAR [28]		incl.	1.031	45	46.4
BELLE [29]		incl.	1.044	78	44.0
HERMES [30]		π^+ (p)	0.980	32	27.8
		π^- (p)	0.980	32	47.8
		π^+ (d)	0.981	32	40.3
		π^- (d)	0.981	32	59.1
COMPASS [31] prel.		π^+ (d)	0.946	199	174.2
		π^- (d)	0.946	199	229.0
PHENIX [21]		π^0	1.112	15	15.8
STAR [33–36]	$0 \leq \eta \leq 1$	π^0	1.161	7	5.7
	$0.8 \leq \eta \leq 2.0$	π^0	0.954	7	2.7
	$\lvert\eta\rvert < 0.5$	$\pi^\pm$	1.071	8	4.3
	$\lvert\eta\rvert < 0.5$	$\pi^+,\pi^-/\pi^+$	1.006	16	17.2
ALICE [32]	7 TeV	π^0	0.766	11	27.7
TOTAL:				973	1154.6

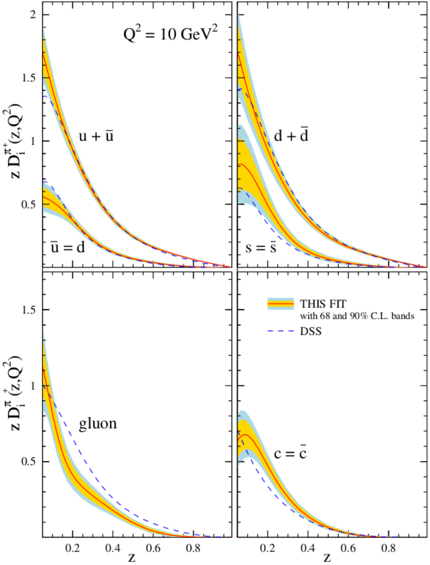

New global DEHSS analysis [PRD 91 (2015) 014035]

How well do we know Fragmentation Functions?

experiment	data type	norm. N_i	# data in fit	χ^2
TPC [37]	incl.	1.003	12	13.4
SLD [33]	incl.	1.014	18	17.2
	uds tag	1.014	10	31.5
	c tag	1.014	10	21.3
	b tag	1.014	10	11.9
ALEPH [30]	incl.	1.026	13	29.7
DELPHI [31]	incl.	1.000	12	6.9
	uds tag	1.000	12	13.1
	b tag	1.000	12	11.0
OPAL [34]	u tag	0.778	5	9.6
	d tag	0.778	5	7.7
	s tag	0.778	5	23.4
	c tag	0.778	5	42.5
	b tag	0.778	5	16.9
BABAR [17]	incl.	1.077	45	30.6
BELLE [18]	incl.	0.996	78	15.6
HERMES [19]	K^+ (p) Q^2	0.843	36	61.9
	K^- (p) Q^2	0.843	36	29.6
	K^+ (p) x	1.135	36	75.8
	K^- (p) x	1.135	36	42.1
	K^+ (d) Q^2	0.845	36	44.7
	K^- (d) Q^2	0.845	36	41.9
	K^+ (d) x	1.095	36	48.9
	K^- (d) x	1.095	36	44.4
COMPASS [22]	K^+ (d)	0.996	309	285.8
	K^- (d)	0.996	309	265.1
STAR [24]	K^+,K^-/K^+	1.088	16	7.6
ALICE [23] 2.76 TeV	K/π	0.985	15	21.6
TOTAL:			1194	1271.7

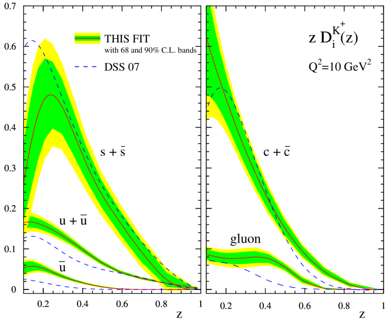

New Global DEHSS analysis [PRD 95 (2017) 094019]

New (SIA-only) analyses

HKKS (B-factory data) [PTEP 2016 (2016) 113B04]

JAM (ITMC methodology) [PRD 94 (2016) 114004]

NNPDF1.0 (neural network, NNLO) [1706.07049]

NNLO [PRD 92 (2015) 114017], low-z resummation [PRD 95 (2017) 054003], HQ [PRD 94 (2016) 034037]

[More in R. Sassot's talk]

A simultaneous determination of FFs and helicity PDFs

1. Perform a simultaneous determination of polarised PDFs and FFs
   from all available data of polarised DIS, polarised SIDIS and SIA

$$d\sigma^{\mathrm{DIS}} = \sum_f d\hat{\sigma}^{\mathrm{DIS}} \otimes \Delta f$$

$$d\sigma^{\mathrm{SIDIS}} = \sum_f d\hat{\sigma}^{\mathrm{SIDIS}} \otimes \Delta f \otimes D_f$$

$$d\sigma^{\mathrm{SIA}} = \sum_f d\hat{\sigma}^{\mathrm{SIA}} \otimes D_f$$

2. Release usual SU(2) and SU(3) constraints used in all other analyses

$$\int_0^1 dx(\Delta u^+ - \Delta d^+) \stackrel{?}{=} g_a$$

$$\int_0^1 dx(\Delta u^+ + \Delta d^+ - s\Delta s^+) \stackrel{?}{=} a_8$$

3. Use the Iterative Monte Carlo fitting procedure
   statistically sound representation of experimental uncertainties
   avoid potential biases introduced by fixing parameters not well constrained by the data

Fit quality and strangeness [arXiv:1705.05889, see also N. Sato's talk]

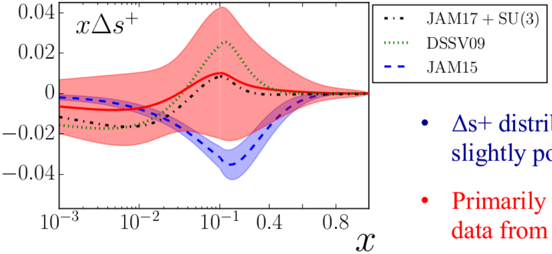

- Δs+ distribution consistent with zero, slightly positive in intermediate x range
- Primarily influenced by HERMES K- data from deuterium target

process	target	N_{dat}	χ^2
DIS	$p, d, {}^3$He	854	854.8
SIA $(\pi^\pm, K^\pm)$		850	997.1
SIDIS $(\pi^\pm)$			
HERMES	d	18	28.1
HERMES	p	18	14.2
COMPASS	d	20	8.0
COMPASS	p	24	18.2
SIDIS $(K^\pm)$			
HERMES	d	27	18.3
COMPASS	d	20	18.7
COMPASS	p	24	12.3
Total:		**1855**	**1969.7**

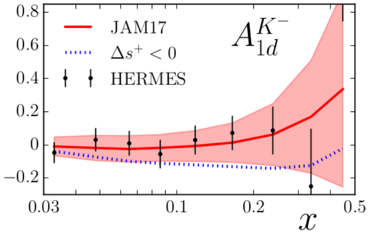

Slide: courtesy of J. Ethier

Moments

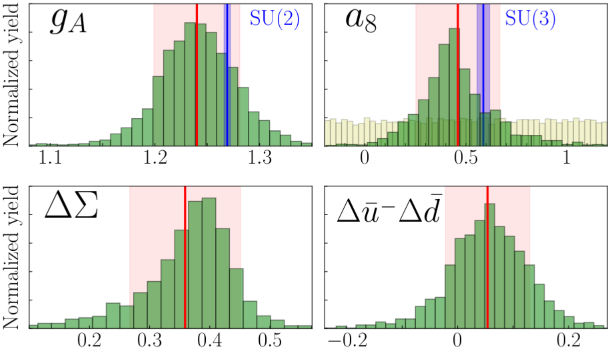

$$g_A = 1.24 \pm 0.04$$ Confirmation of SU(2) symmetry to ~2%

$$a_8 = 0.46 \pm 0.21$$ ~20% SU(3) breaking ± ~20%; large uncertainty

- Need better determination of $\Delta s+$ moment to reduce a_8 uncertainty!

$$\Delta \mathbf{s}^+ = -0.03 \pm 0.09$$

Slide: courtesy of J. Ethier

Moments

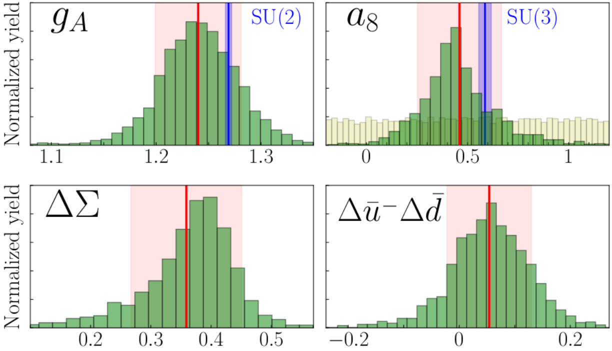

$$\Delta\Sigma = 0.36 \pm 0.09$$

Slightly larger central value than previous analyses, but consistent within uncertainty

Preference for slightly positive sea asymmetry; not very well constrained by SIDIS

$$\Delta\bar{u} - \Delta\bar{d} = 0.05 \pm 0.08$$

Slide: courtesy of J. Ethier

4. Conclusions

Summary

1. Unpolarised PDF: full exploitation of the LHC harvest
   - increased precision over an extended kinematic region
   - theoretical improvements (NNLO, EW corrections, resummations, ...)
   - complementarity with the LHeC and EIC programs

2. Polarised PDFs: only a polarised EIC could provide a significant advancement
   - unprecedented kinematic reach
   - check modified evolution at small x
   - meanwhile, make the most from the RHIC spin physics program

3. Fragmentation Functions: significant phenomneological effort
   - improve the methodological sophistication of current analyses
   - make the most from LHC data
   - non-trivial cross talk between FFs and PDFs requires simultaneous analyses of both

Summary

1. Unpolarised PDF: full exploitation of the LHC harvest
   - increased precision over an extended kinematic region
   - theoretical improvements (NNLO, EW corrections, resummations, ...)
   - complementarity with the LHeC and EIC programs

2. Polarised PDFs: only a polarised EIC could provide a significant advancement
   - unprecedented kinematic reach
   - check modified evolution at small x
   - meanwhile, make the most from the RHIC spin physics program

3. Fragmentation Functions: significant phenomneological effort
   - improve the methodological sophistication of current analyses
   - make the most from LHC data
   - non-trivial cross talk between FFs and PDFs requires simultaneous analyses of both

Thank you